Variation of pore fabric across a fold-thrust structure

Sebastian Pfleiderer, Catherine Kissel

GEOPHYSICAL RESEARCH LETTERS, VOL. 21, NO. 19, PAGES 2147-2150, SEPTEMBER 15, 1994

Variation of pore fabric across a fold-thrust structure

Sebastian Pfleiderer and Catherine Kissel

Centre des Faibles Radioactivités, C.N.R.S.-C.E.A., Gif-sur-Yvette, France

Abstract. Variations of pore orientation, pore shape, porosity, and hydraulic permeability, within a siltstone unit of a fold-thrust structure, are determined using magnetic pore fabric analysis, mercury injection porosimetry, and scanning electron microscopy (SEM). While samples in the foreland show evidence for the preservation of depositional pore geometry, the progressively deformed thrust sheet reveals increasingly oblate pore fabric anisotropy with microcrack planes oriented normal to the tectonic transport direction. Porosity, pore throat sizes, and permeability, show corresponding spatial variations across the structure. Independent of the deformation state within the thrust sheet, pore and magnetic grain fabric correlate closely in orientation.

Introduction

The study of pore fabric is most often motivated by the ambition to link the microgeometry of a porous network to some petrophysical property such as hydraulic or electrical conductivity [*Koplik et al.,* 1984; *Doyen,* 1988]. Situations where such links would be useful include oil and gas production from a reservoir [*Timur,* 1968], geothermal heat recovery [*Rink and Schopper,* 1972], or groundwater flow and contaminant transport [*Katsube,* 1981]. Since these situations frequently involve tectonically deformed, folded or fractured rock, the evolution of pore structure during deformation has been the object of numerous studies.

Deformed pore and fracture networks can be analyzed during controlled deformation experiments in the laboratory, or on field samples of deformed rocks provided the deformation history is well understood. We use here magnetic pore fabric analysis, a technique developed for the study of three-dimensional orientation and shape anisotropy of connected pore spaces [*Pfleiderer and Halls,* 1993], as well as mercury porosimetry and SEM, to determine the microgeometry of connected pores, the spatial distribution of pore fabric, and the variation of pore throat sizes and hydraulic permeability, within a fold-thrust structure. Since the deformation history and the variations of strain state within the chosen structure are well known from microstructural and natural magnetic fabric analyses [*Averbuch et al.,* 1992], we can follow the evolution of pore structure during progressive tectonic deformation. Thus, microcrack formation, porosity alteration, and the resulting change of hydraulic permeability, can be evaluated. At the same time, the paper shows how the method of magnetic pore fabric analysis can be useful in analyzing the three-dimensional porous structure of sedimentary rock of low hydraulic permeability.

Paper number 94GL01907
0094-8534/94/94GL-01907$03.00

Sampling and Measurement Strategy

We use samples of a previous field study, which describes the deformation state of one depositional unit at several sites across the Lagrasse structure (Corbières, NE Pyrenees) [*Averbuch et al.,* 1992]. (For geological descriptions, maps, and sampling locations see this reference.) Sites are situated in the foreland, the hinterland, and at the hinge zone, including roof limb, hinge, and forelimb, thus covering the entire structure. Samples comprise Paleocene fluvial, non-metamorphosed siltstones containing various amounts of quartz, calcite, kaolinite, illite and hematite. They were deformed first by layer-parallel shortening (LPS), causing a vertical macro-cleavage, and an alignment of clay minerals and hematite parallel to this cleavage, then by the folding and displacement of the thrust sheet. While samples from the foreland show only signs of moderate internal deformation due to the LPS event, the front of the thrust sheet is affected additionally by folding [*Averbuch et al.,* 1992]. The back of the structure, displaced as a rigid body during the thrusting event, displays normal faulting due to a subsequent period of extensional deformation.

The method of magnetic pore fabric analysis is described, and applied to the study of porous sandstones of high hydraulic permeability (> 1 mDarcy), by *Pfleiderer and Halls* [1993]. It consists of measurements of the anisotropy of magnetic susceptibility (AMS) of samples impregnated with a magnetic colloid. Results can be directly interpreted in terms of average directions of pore alignment and pore shape ratios, provided that bulk susceptibility, $\bar{k}$, of the impregnated sample exceeds natural susceptibility. (As shown in the following sections, $\bar{k}$ exceeds the value of natural susceptibility by two to three orders of magnitude.) Since the technique requires complete and homogeneous impregnation of specimens with the colloid, samples have to be sufficiently permeable, and pore throats large enough, to allow for passage of the colloid, and of suspended magnetite particles, throughout the porous network. The threshold of minimum permeability and pore throat size, below which the impregnation of specimens becomes impossible, is unknown at present. The examination of low permeability siltstones is therefore a test of the limits of applicability of magnetic pore fabric analysis.

To study the relationship between magnetic grain and pore fabric, we measure natural AMS for each sample before impregnation. Thus, rock deformation can be observed at the same time as pore evolution, and the effect of grain rotation, redistribution, or neomineralization, on pore alteration can be demonstrated.

For some of the samples, we carried out mercury porosimetry experiments to determine the amount of connected porosity, the distribution of pore throat sizes, and to estimate bulk hydraulic permeability, using a model based on percolation theory [*Katz and Thompson,* 1987]. In combination

with the results from magnetic pore fabric analysis, it becomes possible to evaluate the relative proportion of pores and cracks of the samples.

Finally, SEM observations are used to verify pore diameters and crack widths obtained from mercury porosimetry, and to analyze pore geometry in detail. Furthermore, SEM images of back-scattered electrons allow for the identification of magnetic material crystallized within pore spaces.

Spatial distribution of pore fabric across the structure

Orientation of pore fabric

Figure 1 illustrates the variations of pore fabric orientation across the Lagrasse structure. Orientation of pore fabric is expressed by the direction of maximum (k_{max}) and minimum (k_{min}) axes of the AMS ellipsoid measured on impregnated samples (filled symbols). The natural magnetic fabric of the samples before impregnation is shown for comparison (hollow symbols). Each ellipsoid represents a tensor average of n samples (Figure 1). To evaluate the variations within a site, we project elliptical cones of 95% confidence around each axis. Results of principal directions are corrected for sample orientation, and refer to geographic North. Bedding plane orientations (s_0) are given in Figure 1 to show the directions of principal axes with respect to bedding.

In the foreland, minimum axes are oriented horizontally North-South. The large cones of 95% confidence indicate that pore fabric is weakly defined in this region. Furthermore, a large angular difference (62°) occurs at this site between maximum axes of the average ellipsoids before and after sample impregnation. This difference is not only due to averaging of widely scattered AMS orientations because individual specimens show a similar deviation between magnetic grain and pore fabric. The natural magnetic fabric displays a foliation plane which coincides in orientation with a vertical, East-West trending macro-cleavage, noticed in the field, and resulting from layer-parallel shortening [*Averbuch et al.* 1992]. The well defined orientation of k_{min} of natural samples demonstrates the effect of rearrangement of magnetic grain fabric, while the wide scattering of pore fabric may indicate a transitional state where reorganization of the original porous structure has not yet been completed.

Within the thrust sheet, all sites show minimum axes parallel to the tectonic transport direction (towards Northwest), inclined by 20°-40°. Narrow regions of confidence demonstrate that orientations remain effectively constant within each site. The directions of principal axes show no correlation with the changes in bedding attitude, indicating that any pre-deformational fabric has been entirely overprinted by the deformation. Furthermore, pore and magnetic grain fabric correspond closely in orientation at any one site and for any one sample individually, which shows that deformation of grains and matrix, and alteration of voids, are not independent at higher states of deformation. Our results reveal that progressive deformation has lead to coinciding orientations of pore and magnetic grain fabric within the Lagrasse thrust sheet.

Anisotropy parameters

Figure 2 shows axial ratios of the ellipsoids of Figure 1, plotted on Flinn-diagrams. Except for the results in the foreland, all diagrams display oblate ellipsoid shapes with magnetic foliation, k_{int}/k_{min}, of impregnated samples exceeding the ratio for natural samples. The site in the foreland is characterized by a weakly anisotropic natural magnetic fabric, and by prolate pore fabric anisotropy, which again

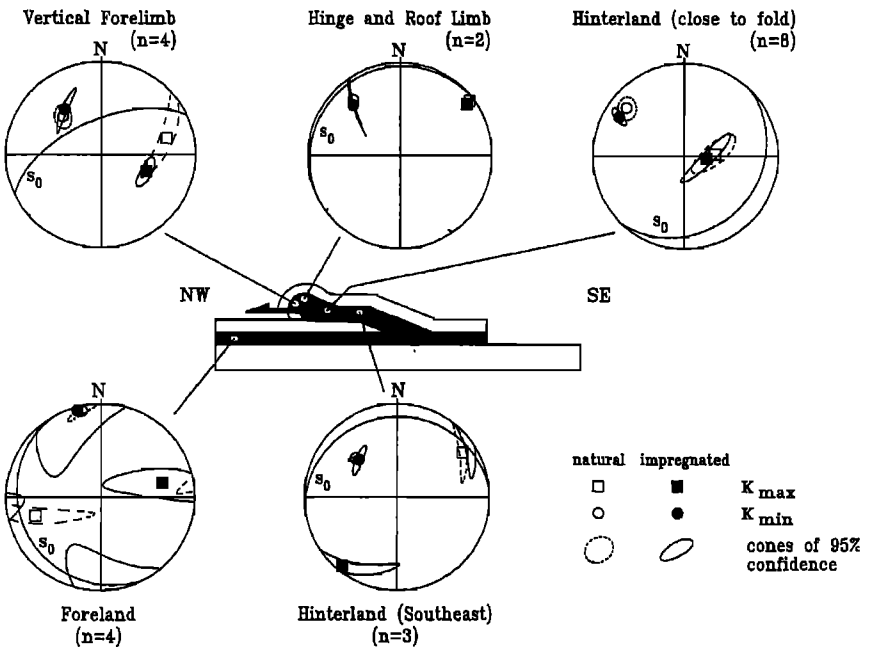

Figure 1. Spatial distribution of the orientation of magnetic grain and pore fabric across the Lagrasse structure. Lower-hemisphere, equal-area projections of maximum and minimum axes of AMS ellipsoids measured before and after sample impregnation. Anisotropies of natural and impregnated samples are interpreted in terms of magnetic grain and pore fabric, respectively. Each ellipsoid represents a tensor average of n samples, elliptical cones of 95% confidence are projected around each axis, s_0 marks the bedding plane orientation.

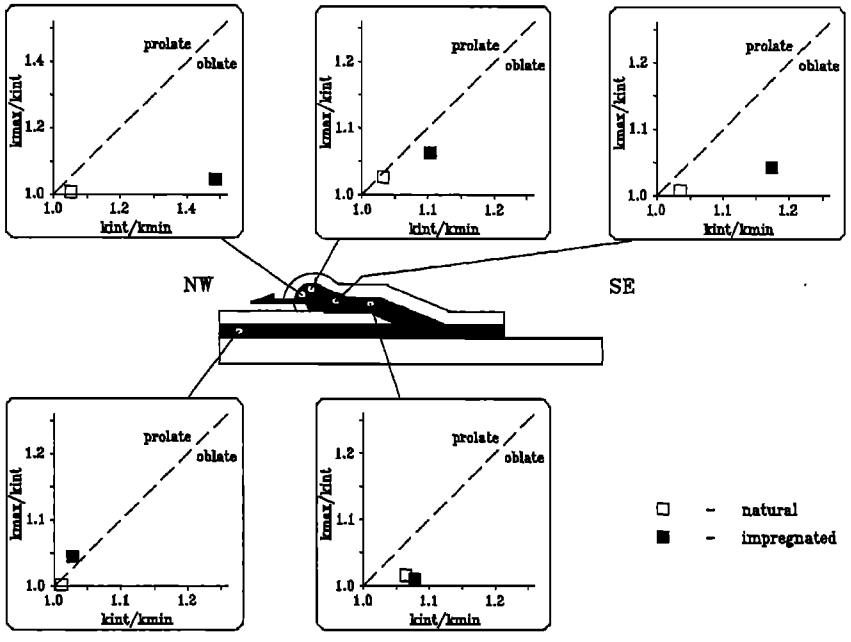

Figure 2. Spatial distribution of parameters of magnetic grain and pore fabric anisotropy across the Lagrasse structure. Axial ratios of the ellipsoids of Figure 1.

indicates the transitional state of pore structural organization with possible interference between inherited depositional and newly forming tectonic fabric.

Approaching the frontal fold from the south-east, we observe an increase of magnetic foliation, which can be interpreted by the flattening of pore spaces through progressive deformation. (Note the change of scale for the Flinn-diagram at the vertical forelimb.) However, this increase can also be explained by the gradual formation of microcracks. (We will confirm this second interpretation later with the aid of mercury porosimetry results and SEM observations.) The orientation of these microcracks can be derived from Figure 1 since the minimum axis of the AMS ellipsoid is normal to the planes of microcracks. Except for the site at the vertical forelimb, the microcracks observed with the AMS method are parallel to the macro-cleavage observed in the field.

Table 1 lists the degrees of anisotropy, $P = k_{max}/k_{min}$, of impregnated samples. Since the inverse of this ratio corresponds to the aspect ratio (width / length) of microcracks, large P values indicate long, narrow cracks, while values closer to 1.0 imply wide open cracks or more isotropic pore shapes. The spatial distribution of P correlates with the variations seen in Figure 2, showing the lowest value in the foreland and a gradual increase from the south-east towards the front region of the thrust-fold. This trend is slightly interrupted by a lower value of P at the hinge.

The magnitudes of bulk magnetic susceptibility of impregnated samples are listed in Table 1 and defined as $\bar{k} = (k_{max}+k_{int}+k_{min})/3$. Similar to the confidence cones in Figure 1, the standard deviations of $\bar{k}$ indicate the data spread within a site. $\bar{k}$ directly reflects the amount of magnetic colloid injected into the sample, and is therefore proportional to the value of connected porosity [*Pfleiderer*, 1992]. The highest bulk susceptibilities are found at the site furthermost to the Southeast and at the hinge and horizontal roof limb. These two sites were subjected to extensional deformation, the former during the period following the thrusting event, the latter during the folding. The resulting opening of microcracks causes porosity to increase, and P to decrease, at these locations, which is supported by our measurements.

Table 1. Degree of anisotropy ($P = k_{max}/k_{min}$), bulk magnetic susceptibility ($\bar{k} = (k_{max}+k_{int}+k_{min})/3$), its standard deviation (σ_k), connected porosity (ϕ), range of pore throat apertures (d_{min}-d_{max}), and bulk hydraulic permeability (K_{hyd}), of impregnated samples of the Lagrasse structure. Location of sites as illustrated in Figures 1 and 2.

	Foreland	Hinterland		Hinge Zone	
		furthermost to the Southeast	close to the frontal fold	horizontal roof limb and hinge	vertical forelimb
P	1.07	1.09	1.23	1.17	1.56
$\bar{k}$ (S.I.-units)	2.75×10^{-3}	33.6×10^{-3}	9.94×10^{-3}	11.1×10^{-3}	6.03×10^{-3}
σ_k (S.I.-units)	2.4×10^{-5}	2.5×10^{-3}	7.6×10^{-4}	4.3×10^{-4}	1.2×10^{-4}
ϕ (Percent)	2.2	5.7	3.7	-	3.7
d_{min}-d_{max} (μm)	0.01 - 0.1	0.1 - 10.0	0.01 - 1.0	-	0.01 - 1.0
K_{hyd} (μDarcy)	0.05	121	0.7	-	1.2

Results from mercury porosimetry and SEM

Mercury injection porosimetry, carried out for samples in the foreland, the hinterland, and at the vertical forelimb, reveals connected porosity, ϕ, and ranges of pore throat apertures, d_{min}-d_{max}, as listed in Table 1. Porosity, determined from the volume of mercury injected at maximum pressure (400 MPa), and pore throat sizes, computed using the Washburn-equation [*Washburn,* 1921], show the same tendency of variation as $\bar{k}$, with the lowest values in the foreland and maxima in the Southeast.

Trapped porosity, given by the amount of mercury remaining within the sample after pressure relaxation, ranges between 35% and 53% of total connected porosity. Because of the homogeneous distribution of pore throat sizes, revealed by the mercury injection measurements, these values seem to indicate that the porosity of our samples consists predominantly of microcracks [*Wardlaw et al.,* 1988]. This observation agrees with the highly oblate shape of AMS ellipsoids.

Bulk hydraulic permeability, K_{hyd}, of our samples ranges from 0.05 to 121 μDarcy (Table 1). For the estimation of K_{hyd}, we use the model of *Katz and Thompson* [1987] based on percolation theory. According to this model, a threshold pressure, at which the injected mercury forms the first continuous path across the sample, determines a characteristic pore throat size from which K_{hyd} is calculated. Since K_{hyd} is proportional to the pore throat size and to ϕ, the variation of permeability across the structure closely follows the distribution of pore apertures and of connected porosity, with the lowest value in the foreland and a maximum at the site furthermost to the Southeast (Table 1).

SEM analyses of samples from the thrust sheet, confirm that microcracks make up most of the porosity. Furthermore, analysis of back-scattered electron images demonstrate that most of the iron oxide grains, causing the natural magnetic fabric and identified as hematite by *Averbuch et al.* [1992], are located within, and often parallel to, crack planes. This may explain the close correspondence in principal directions of AMS ellipsoids before and after sample impregnation, seen in Figure 1.

Conclusions

Visual inspection of the impregnation state at the specimens' centre after AMS determination, as well as the values of bulk susceptibility after impregnation, prove the successful impregnation of our samples. Furthermore, $\bar{k}$ exceeds the value of natural susceptibility by 2 to 3 orders of magnitude. Therefore, the technique of magnetic pore fabric analysis appears to be applicable to siltstones of low hydraulic permeability ($K_{hyd} \geq 0.05$ μDarcy) and narrow pore throats ($d_{min} \geq 0.01$ μm).

While the original pore fabric in the foreland remains partially unaffected by the deformation, the transport of the structure towards the Northwest has generated microcracks within the entire thrust sheet. The orientation of these microcracks, normal to the direction of minimum susceptibility, is independent from the structural attitude of the depositional unit. Any pre-deformational fabric becomes overprinted during the deformation.

In the hinterland furthermost to the Southeast, microcracks open during a period of extension following the emplacement of the thrust-fold, causing high permeability, high porosity, and a reduced degree of anisotropy. The samples at the hinge zone, and in the hinterland close to the frontal fold, do not develop open cracks, possibly due to continuing compression or filling through neomineralization. The foreland shows little or no sign of fracturing, narrow pore apertures, and the lowest values of porosity and hydraulic permeability.

Moreover, the study of pore and magnetic grain fabric evolution shows the interdependence between the deformation of grains and matrix, and the alteration of voids. Our results suggest that hematite grains may have newly grown within, or rotated into a position parallel to, the microcracks, giving rise to identical orientations of natural magnetic fabric and AMS of impregnated samples within the thrust sheet. Orientations do not coincide in the weakly deformed foreland, possibly due to incomplete reorganization of grains and pore structure.

Acknowledgments. We thank J.-F. Tannau for manufacturing of the sample impregnation device; J. Maury (C.E.A., Saclay) for the mercury porosimetry analyses; J. Phalippou (Université d'Orsay) and L. Froget (C.E.A., Gif-sur-Yvette) for the SEM work; H. C. Halls (University of Toronto), R. Panozzo Heilbronner (Universität Basel), and an anonymous reviewer for critical comments. S.P. was financially supported by an EC research fellowship. This is CFR contribution No. 1627.

References

Averbuch, O., D. Frizon de Lamotte, and C. Kissel, Magnetic fabric as a structural indicator of the deformation path within a fold-thrust structure: a test case from the Corbières (NE Pyrenees, France), *J. Struct. Geol., 14,* 461-474, 1992.

Doyen, P. M., Permeability, conductivity and pore geometry of sandstone, *J. Geophys. Res., 93,* 7792-7740, 1988.

Katsube, T. J., Pore structure and pore parameters that control the radionuclide transport in crystalline rocks, *Proc. of the Technical Program, Int. Powder and Bulk Solids Handling and Processing, Rosemount, Illinois,* 394-409, 1981.

Katz, A. J., and A. H. Thompson, Prediction of rock electrical conductivity from mercury injection measurements, *J. Geophys. Res., 92,* 599-607, 1987.

Koplik, J., C. Lin, and M. Vermette, Conductivity and permeability from microgeometry, *J. Appl. Phys., 56,* 3127-3131, 1984.

Pfleiderer, S., Magnetic pore fabric analysis, Ph.D. thesis, 104 pp., University of Toronto, Toronto, Ont., June 1992.

Pfleiderer, S., and H. C. Halls, Magnetic pore fabric analysis: verification through image autocorrelation, *J. Geophys. Res., 98,* 4311-4316, 1993.

Rink, M., and J. R. Schopper, Pore structure and physical properties of porous sedimentary rocks, *Pure Appl. Geophys., 114,* 273-284, 1972.

Timur, A., An investigation of permeability, porosity, & residual water saturation relationships for sandstone reservoirs, *The Log Analyst, 9,* 8-17, 1968.

Wardlaw, N. C., M. McKellar, and Y. Li, Pore and throat distributions determined by mercury injection porosimetry and direct observation, *Carbonates and Evaporites, 3,* 1-15, 1988.

Washburn, E. W., Note on a method of determining the distribution of pore sizes in a porous material, *Proc. Nat. Acad. Sci. U.S.A., 7,* 115-116, 1921.

S. Pfleiderer and C. Kissel, Centre des Faibles Radioactivités, Laboratoire Mixte C.N.R.S.-C.E.A., Avenue de la Terrasse, 91198 Gif-sur-Yvette Cedex, France

(Received January 17, 1994; revised April 28, 1994; accepted July 1, 1994.)